10.24425/acs.2026.1538

Archives of Control Sciences
Volume 36(LXXII), 2026
No. 2*, pages 277–302*

A new 4-D hyperchaotic two-scroll system with two unstable equilibrium points, its dynamic analysis, circuit simulation and synchronization design via integral sliding mode control

Sundarapandian VAIDYANATHAN, Fareh HANNACHI, Mohamad Afendee MOHAMED, Aceng SAMBAS and Manikonda Srinivasa SESHA SAI

In this research work, a new hyperchaotic two-scroll system with two unstable equilibrium points has been derived and the qualitative properties of the new hyperchaotic system are detailed. A bifurcation analysis has been carried out for the proposed hyperchaotic two-scroll system by varying the system parameters. Multistability property of the new hyperchaotic two-scroll system has been also illustrated by showing the coexistence of hyperchaotic attractors for the proposed hyperchaotic two-scroll system for the same set of parameter values but different initial conditions. For engineering applications, we provide an electronic circuit simulation of the proposed hyperchaotic two-scroll system using MultiSim 14.0. As a control application, we derive new results for the complete synchronization for a pair of new hyperchaotic two-scroll systems taken as the master and slave systems. We have used integral sliding mode control and Lyapunov stability theory for the derivation of the synchronizing control law for the complete

S. Vaidyanathan (corresponding author, e-mail: sundarvtu@gmail.com) is with Centre for Control Systems, Vel Tech University, 400 Feet Outer Ring Road, Avadi, Chennai-600062, Tamil Nadu, India and Faculty of Information and Computing, Universiti Sultan Zainal Abidin, Gong Badak, 21300, Terengganu, Malaysia.

F. Hannachi (e-mail: fareh.hannachi@univ-tebessa.dz) is with Larbi Tebessi University – Tebessi, Route de Constantine, 12022, Tebessa, Algeria

M.A. Mohamed (e-mail: mafendee@unisza.edu.my) is with Faculty of Information and Computing, Universiti Sultan Zainal Abidin, Gong Badak, 21300, Terengganu, Malaysia.

A. Sambas (e-mails: acengsambas@unisza.edu.my, acengs@umtas.ac.id) is with Faculty of Informatics and Computing, Universiti Sultan Zainal Abidin, Gong Badak, 21300, Terengganu, Malaysia and Department of Mechanical Engineering, Universitas Muhammadiyah Tasikmalaya, Jawa Barat 46196, Indonesia.

M.S. Sesha Sai (e-mail: dr.msssai.cse@kitsguntur.ac.in) is with Department of Information Technology, KKR & KSR Institute of Technology and Sciences, Guntur-522017, Andhra Pradesh, India.

Received 3 September 2025.

synchronization design for a pair of new hyperchaotic two-scroll systems. We have provided MATLAB simulations to illustrate and highlight the main results of this work.

Key words: chaos, chaotic systems, curve equilibrium, bifurcation, multistability, circuit design, synchronization, sliding mode control

1. Introduction

Nonlinear systems of differential equations are called as hyperchaotic systems if they are equipped with at least two positive Lyapunov exponents [1]. Hyperchaotic systems with high complexity have several applications in science, engineering and technology such as memristors [2, 3], robotics [4, 5], oscillators [6, 7], fuzzy systems [8, 9], finance systems [10, 11], cryptosystems [12–14], etc.

In the chaos literature, several hyperchaotic systems have been reported with various properties such as two-scroll systems [15, 16], four-scroll systems [17, 18], multi-scroll systems [19, 20], systems with hidden attractors [21, 22], etc.

In this research work, a new hyperchaotic two-scroll system with two unstable equilibrium points has been derived and the qualitative properties of the new hyperchaotic two-scroll system are detailed. The proposed hyperchaotic system has a total of four quadratic nonlinearities. We show that the new hyperchaotic system exhibits the Lyapunov exponents $l_1 = 3.4070$, $l_2 = 0.1194$, $l_3 = 0$ and $l_4 = -29.5256$. Since the proposed system has two positive Lyapunov exponents, the system is hyperchaotic. Since the sum of the Lyapunov exponents is negative, the proposed hyperchaotic system is dissipative. A bifurcation analysis has been carried out for the proposed hyperchaotic two-scroll system by varying the system parameters. Bifurcation analysis is very useful for understanding the qualitative properties of the dynamical systems [22, 23].

In chaos theory, multistability refers to the property of coexistence of chaotic or hyperchaotic attractors for the same set of values of system parameters but different values of the initial conditions [24–26]. In this research work, we establish the multistability property of the new hyperchaotic two-scroll system by demonstrating the coexistence of hyperchaotic attractors for the proposed hyperchaotic two-scroll system for the same set of parameter values but different initial conditions.

It is well-known that the design of electronic circuits for chaotic and hyperchaotic systems is very useful for the engineering applications [27, 28]. In this research work, we provide an electronic circuit simulation of the proposed hyperchaotic two-scroll system using MultiSim 14.0.

As a control application, we derive new results for the complete synchronization for a pair of new hyperchaotic two-scroll systems taken as the master and slave systems. Complete synchronization (CS) is a phenomenon where two chaotic or hyperchaotic systems consisting of a master drive system and a slave response system converge to the exact same trajectory over time [29,30]. Synchronization of hyperchaotic systems has important applications in secure communication systems [31,32]. In this research work, we have used integral sliding mode control for the derivation of the synchronizing control law for the complete synchronization design for a pair of new hyperchaotic two-scroll systems. Integral sliding mode control (ISMC) is an useful control technique for the synchronization of hyperchaotic systems [33–35]. We have provided MATLAB simulations to illustrate and highlight the main results of this work.

2. A new hyperchaotic two-scroll system with four quadratic nonlinearities

In this research paper, we propose a new 4-D dynamics given by

$$\begin{cases} \dot{y}_1 = a(y_2 - y_1) - y_2^2 + p y_2 y_3 \,, \\ \dot{y}_2 = b y_1 - y_1 y_3 + y_4 \,, \\ \dot{y}_3 = y_1 y_2 - c y_3 \,, \\ \dot{y}_4 = y_1 \,, \end{cases} \tag{1}$$

where $a, \; b, \; c, \; p$ are positive bifurcation parameters and $Y = (y_1, y_2, y_3, y_4)$ is the state vector.

We shall establish that the 4-D system (1) with a total of four quadratic nonlinearities will exhibit a hyperchaotic attractor when the system constants take the following values

$$a = 24, \quad b = 18, \quad c = 2, \quad p = 14. \tag{2}$$

For numerical simulations, we assume the initial state as $Y(0) = (0.5, 0.3, 0.5, 0.3)$ and the parameters as $(a, b, c, p) = (24, 18, 2, 14)$. Using MATLAB, the Lyapunov exponents (LEs) for the 4-D dynamics (1) can be calculated for these values with $T = 1 \times (10)^4$ seconds as follows:

$$l_1 = 3.4070, \quad l_2 = 0.1194, \quad l_3 = 0, \quad l_4 = -29.5256. \tag{3}$$

Since the 4-D dynamics (1) has two positive LE values, we deduce that the 4-D system (1) has a hyperchaotic attractor with the maximal Lyapunov exponent (MLE) equal to $l_{\max} = 3.4070$, which is a high value. Thus, the proposed hyperchaotic system (1) exhibits high complexity and hence it can be used for applications in encryption and secure communications. Moreover, the Lyapunov dimension for the 4-D hyperchaotic system (1) is determined as follows:

$$D_L = 3 + \frac{l_1 + l_2 + l_3}{|l_4|} = 3.1194 \tag{4}$$

which exhibits the high complexity of the proposed hyperchaotic system (1). The rest points of the new hyperchaotic system (1) are got by means of solving the following set of equations:

$$a(y_2 - y_1) - y_2^2 + py_2y_3 = 0, \tag{5a}$$

$$by_1 - y_1y_3 + y_4 = 0, \tag{5b}$$

$$y_1y_2 - cy_3 = 0, \tag{5c}$$

$$-y_1 = 0. \tag{5d}$$

From (5d), (5c) and (5b), we find that $y_1 = 0$, $y_3 = 0$ and $y_4 = 0$. Substituting these values in (5a), we get $ay_2 - y_2^2 = 0$ or $y_2(a - y_2) = 0$. This calculation shows that the new 4-D hyperchaotic system (1) has two equilibrium points, viz. $P_0 = (0, 0, 0, 0)$ and $P_1 = (0, a, 0, 0)$

For the hyperchaotic case $(a, b, c, p) = (24, 18, 2, 14)$, we find that $a = 24$. Thus, the equilibrium points of the system (1) in the hyperchaotic case are $P_0 = (0, 0, 0, 0)$ and $P_1 = (0, 24, 0, 0)$.

The Jacobian matrix of the system (1) at $P_0 = (0, 0, 0, 0)$ is found as

$$M_0 = \begin{bmatrix} -a & a & 0 & 0 \\ b & 0 & 0 & 1 \\ 0 & 0 & -c & 0 \\ -1 & 0 & 0 & 0 \end{bmatrix}. \tag{6}$$

It is clear that $\lambda = -c$ is a stable eigenvalue of M_0 as $c > 0$, while the other three eigenvalues are the roots of the equation

$$\varphi(\lambda) = \lambda^3 + a\lambda^2 - ab\lambda + 1 = 0. \tag{7}$$

Since $a > 0$ and $b > 0$, it is clear from the Routh's stability criterion that the cubic polynomial $\varphi(\lambda)$ is unstable.

From Descarte's rule of signs, we can also deduce that $\varphi(\lambda)$ has two positive real roots and one negative real root.

Hence, $P_0 = (0, 0, 0, 0)$ is a saddle point and unstable equilibrium of the 4-D system (1) when $a > 0$, $b > 0$ and $c > 0$.

The Jacobian matrix of the system (1) at $P_1 = (0, a, 0, 0)$ is found as

$$M_1 = \begin{bmatrix} -a & -a & pa & 0 \\ b & 0 & 0 & 1 \\ a & 0 & -c & 0 \\ -1 & 0 & 0 & 0 \end{bmatrix}. \tag{8}$$

For the hyperchaotic case (2), we can simplify the Jacobian matrix M_1 as

$$M_1 = \begin{bmatrix} -24 & -24 & 336 & 0 \\ 18 & 0 & 0 & 1 \\ 24 & 0 & -2 & 0 \\ -1 & 0 & 0 & 0 \end{bmatrix}. \tag{9}$$

Using MATLAB, we compute the eigenvalues of the Jacobian matrix M_1 as $74.99, -101.11$ and $0.06 \pm 0.06i$. This shows that P_1 is an unstable, saddle-focus, equilibrium of the 4-D hyperchaotic two-scroll system (1).

MATLAB simulations for the new 4-D hyperchaotic two-scroll system (1) for the initial state $(0.5, 0.3, 0.5, 0.3)$ and $(a, b, c, p) = (24, 18, 2, 14)$ are presented in Figures 1 to 4.

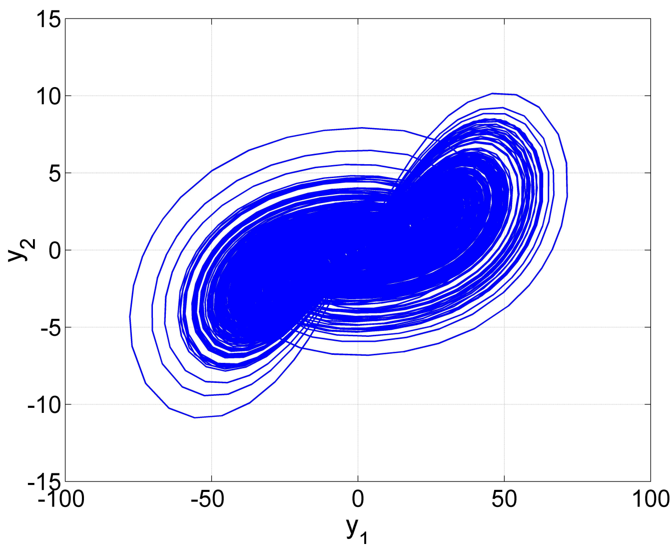

Figure 1: (y_1, y_2) plot of the new hyperchaotic two-scroll system (1) for $Y(0) = (0.5, 0.3, 0.5, 0.3)$ and $(a, b, c, p) = (24, 18, 2, 14)$

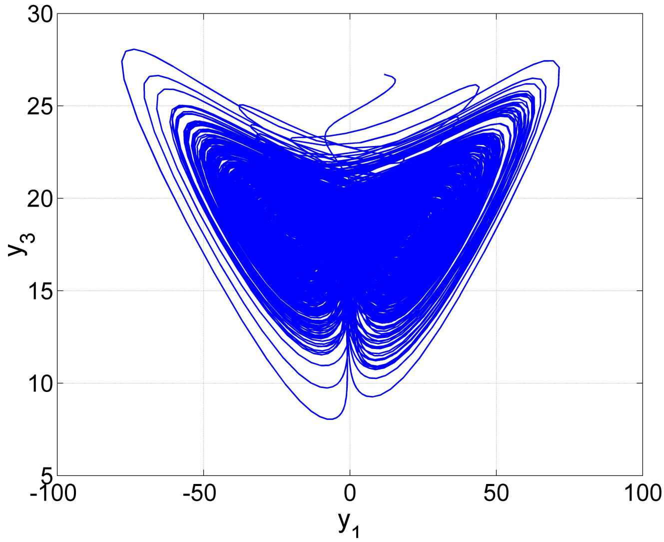

Figure 2: (y_1, y_3) plot of the new hyperchaotic two-scroll system (1) for $Y(0) = (0.5, 0.3, 0.5, 0.3)$ and $(a, b, c, p) = (24, 18, 2, 14)$

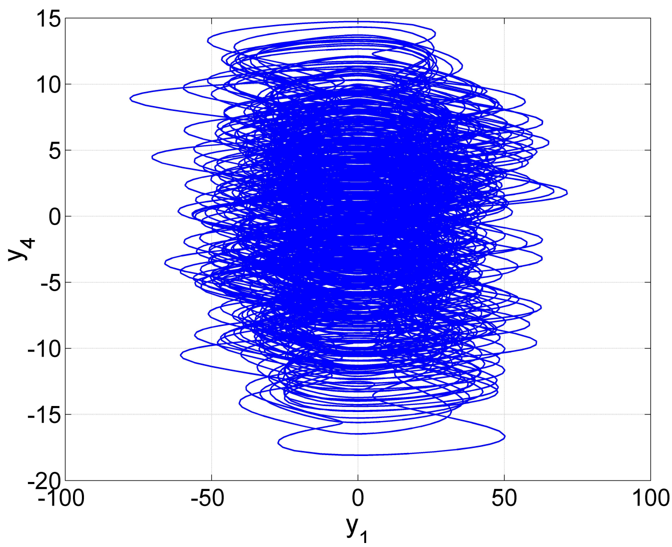

Figure 3: (y_1, y_4) plot of the new hyperchaotic two-scroll system (1) for $Y(0) = (0.5, 0.3, 0.5, 0.3)$ and $(a, b, c, p) = (24, 18, 2, 14)$

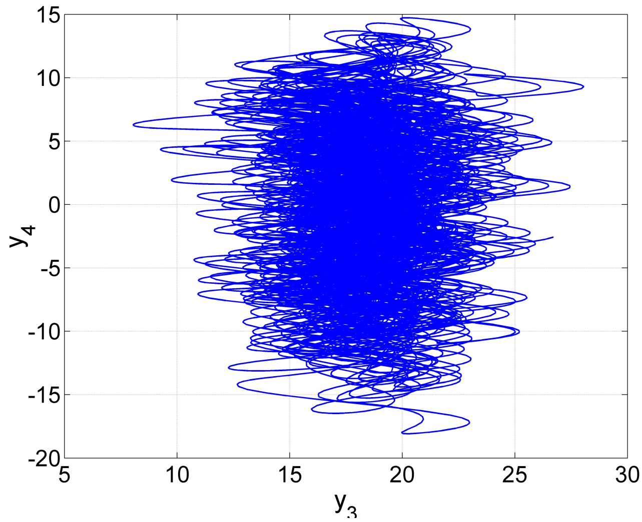

Figure 4: (y_3, y_4) plot of the new hyperchaotic two-scroll system (1) for $Y(0) = (0.5, 0.3, 0.5, 0.3)$ and $(a, b, c, p) = (24, 18, 2, 14)$

3. Dynamic analysis of the new 4-D hyperchaotic two-scroll system

In this section, we carry out a bifurcation analysis of the dynamics of the two-scroll system (1) by means of the bifurcation diagrams and Lyapunov exponents spectrums for the 4-D system (1).

3.1. Varying the parameter a

Here, we fix the values the system parameters (b, c, p) as $(b, c, p) = (18, 2, 14)$ and vary the parameter a in the interval $[20, 30]$. Figure 5 shows the

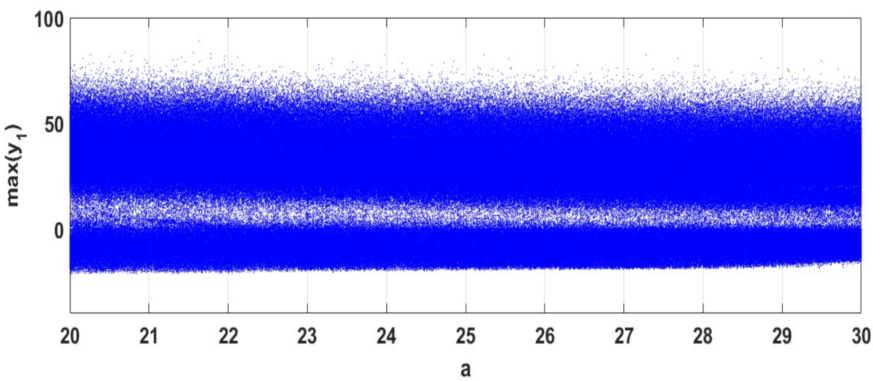

(a)

Fig. 5a

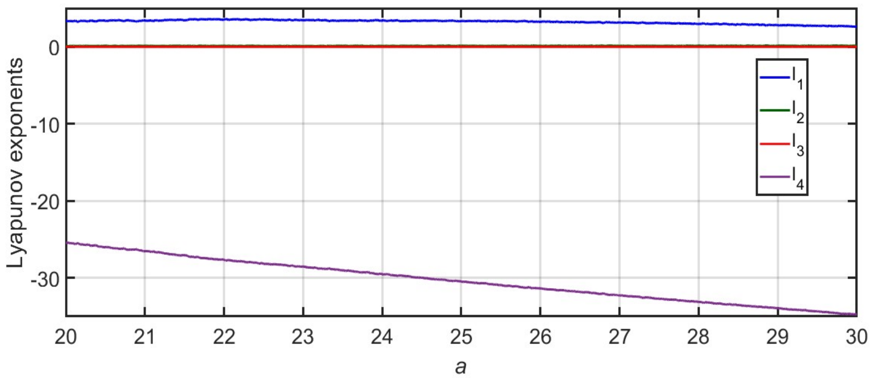

(b)

Figure 5: (a) Bifurcation diagram and (b) LE spectrum of the 4-D two-scroll dynamics (1) for $a \in [20, 30]$ and $(b, c, p) = (18, 2, 14)$

Lyapunov exponents spectrum and the bifurcation diagram of the 4-D system (1) when the parameter a varies in $[20, 30]$ and $(b, c, p) = (18, 2, 14)$.

From Figure 5, it can be seen that the 4-D system (1) exhibits only hyperchaotic behavior when $a \in [20, 30]$, as the system (1) exhibits two positive Lyapunov exponents ($l_1 > 0$, $l_2 > 0$, $l_3 = 0$ and $l_4 < 0$). Behaviors and Lyapunov exponents of the new 4-D system (1) for different values of parameter a are summarized in Table 1.

Table 1: Summary table for the dynamic analysis of the 4-D system (1) for different values of the parameter a and $(b, c, p) = (18, 2, 14)$

Dynamics	Parameter a	LEs			
		l_1	l_2	l_3	l_4
Hyperchaotic	20	3.3410	0.1047	0	−25.4500
	21	3.4080	0	0	−26.5300
	22	3.4940	0.1267	0	−27.6200
	23	3.4380	0.07937	0	−28.5200
	25	3.3030	0.1457	0	−30.4500
	26	3.2480	0.1252	0	−31.3800
	27	3.2120	0.1108	0	−32.3300
	28	2.9720	0.1563	0	−33.1300
	29	2.7560	0.1502	0	−33.9100
	30	2.6100	0.09473	0	−34.7000

3.2. Varying the parameter b

Here, we fix the values the system parameters (a, c, p) as $(a, c, p) = (24, 18, 2)$ and vary the parameter b in the interval $[0, 20]$. Figure 6 shows the Lyapunov exponents spectrum and the bifurcation diagram of the 4-D system (1) when the parameter b varies in $[0, 20]$ and $(a, c, p) = (24, 18, 2)$.

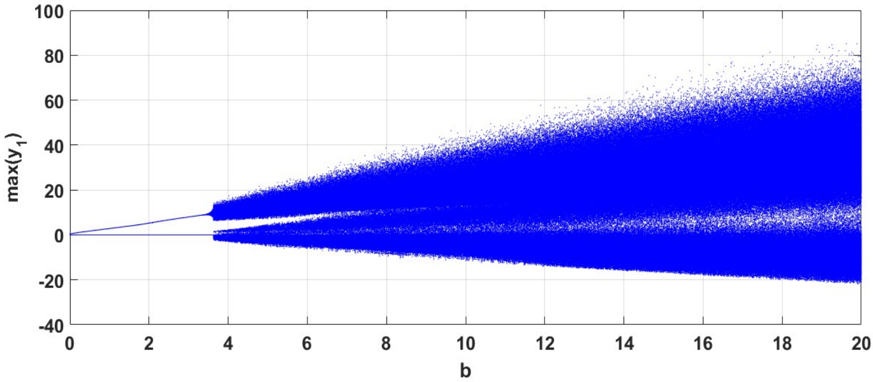

(a)

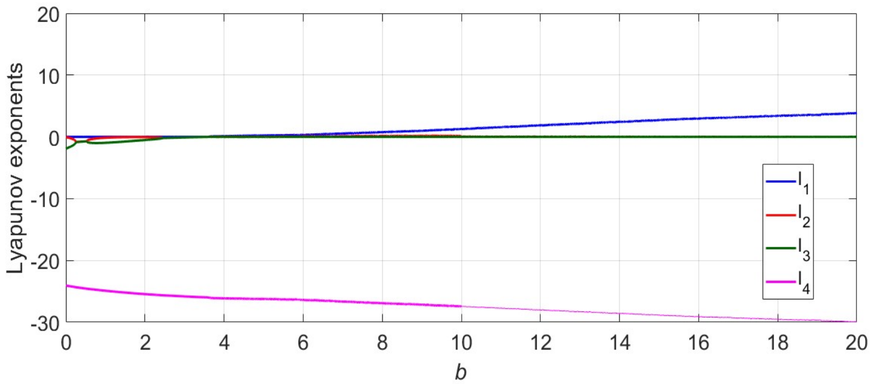

(b)

Figure 6: (a) Bifurcation diagram and (b) LE spectrum of the 4-D two-scroll dynamics (1) for $b \in [0, 20]$ and $(a, c, p) = (24, 18, 2)$

We can identify the dynamic behavior of the system (1), when the parameter b varies in the range $[0, 20]$. We define three regions as follows:

$$A = [0, 2.08) \cup [2.08, 3.62], \quad B = (3.62, 5.32], \quad C = (5.32, 20]. \tag{10}$$

From Figure 6, it can be seen that system (1) exhibits only periodic behavior when $b \in A$, where the maximal Lyapunov exponent is zero and the other

Lyapunov exponents are equal or less than zero. When $b \in B$, we can see from Figure 6 that the system (1) exhibits hyperchaotic and chaotic behavior where one or two Lyapunov exponents are positive, one zero Lyapunov exponent ($l_3 = 0$) and one negative Lyapunov exponent ($l_4 < 0$). Thus, the 4-D system (1) is chaotic and generate chaotic attractor or hyperchaotic attractor when $b \in B$.

When $b \in C$, we can see from Figure 6 that the system (1) has two positive Lyapunov exponents ($l_1 > 0$, $l_2 > 0$), one zero Lyapunov exponent ($l_3 = 0$) and one negative Lyapunov exponent ($l_4 < 0$). Thus, the system (1) is hyperchaotic and generates a hyperchaotic attractor, when $b \in C$.

Behaviors and Lyapunov exponents of the new 4-D two-scroll system (1) for different values of parameter b are summarized in Table 2.

Table 2: Summary Table for the dynamic analysis of the 4-D system (1) for different values of the parameter b and $(a, c, p) = (24, 18, 2)$

Dynamics	Parameter b	LEs			
		l_1	l_2	l_3	l_4
Periodic	0	0	−0.0431	−1.9020	−24.050
	0.5	0	−0.7181	−0.7324	−24.54
	1.2	0	−0.08904	−0.8853	−25.02
	2	0	−0.04332	−0.5120	−24.45
	2.50	0	−0.1720	−0.1782	−25.65
	3	0	0	−0.08935	−25.82
	3.50	0	−0.01993	−0.01815	−25.96
Chaotic	4.60	0.1959	0	−0.01069	−26.19
Hyperchaotic	3.84	0.09679	0.01834	0	−26.10
	4	0.09521	0.0287	0	−26.12
	5	0.2253	0.01994	0	−26.25
	5.50	0.04781	0.04781	0	−26.29
	8	0.7535	0.1493	0	−26.90
	12	1.8760	0.1300	0	−28.00
	15	2.7290	0.1225	0	−28.86
	17	3.1670	0.1292	0	−29.52
	20	3.865	0.09552	0	−29.96

3.3. Varying the parameter c

Here, we fix the values the system parameters (a, c, p) as $(a, b, p) = (24, 18, 14)$ and vary the parameter c in the interval $[0, 10]$. Figure 7 shows the Lyapunov exponents spectrum and the bifurcation diagram of the 4-D system (1) when the parameter c varies in $[0, 10]$ and $(a, b, p) = (24, 18, 14)$.

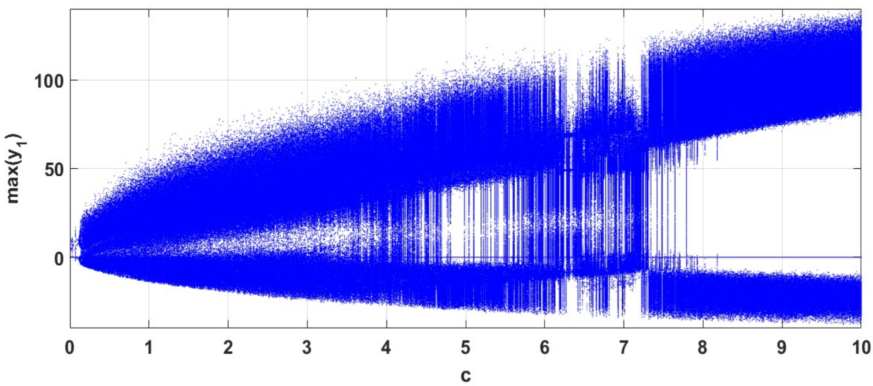

(a)

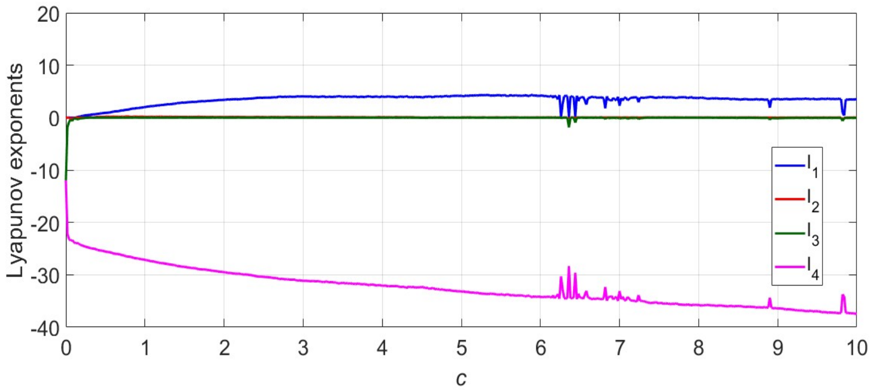

(b)

Figure 7: (a) Bifurcation diagram and (b) LE spectrum of the 4-D two-scroll dynamics (1) for $c \in [0, 10]$ and $(a, b, p) = (24, 18, 14)$

We can identify the dynamic behavior of the system (1), when the parameter c varies in the range $[0, 10]$. We define three regions as follows:

$$A = (0, 0.04) \cup (0.12, 0.28)\,, \quad B = [0.04, 0.12]\,, \quad C = [0.28, 10]\,. \qquad (11)$$

When $c \in A$, we can see from Figure 7 that the system (1) exhibits chaotic behavior where $l_1 > 0$, $l_2 = 0$, $l_3 < 0$ and $l_4 < 0$. Thus, the system (1) is chaotic and generates a chaotic attractor, when $c \in A$.

When $c \in B$, we can see from Figure 7 that the system (1) exhibits only periodic behavior because the maximal Lyapunov exponent is zero and the other Lyapunov exponents are less than or equal to zero.

When $c \in C$, we can see from Figure 7 that the system (1) exhibits hyperchaotic behavior where $l_1 > 0$, $l_2 > 0$, $l_3 = 0$ and $l_4 < 0$. Thus, the system (1) is hyperchaotic and generates a hyperchaotic attractor, when $c \in C$.

Behaviors and Lyapunov exponents of the new 4-D system (1) for different values of parameter c are summarized in Table 3.

Table 3: Summary Table for the dynamic analysis of the 4-D system (1) for different values of the parameter c and $(a, b, p) = (24, 18, 14)$

Dynamics	Parameter	LEs			
	c	l_1	l_2	l_3	l_4
Periodic	0.04	0	−01358	−0.8389	−23.19
	0.05	0	−0.1822	−0.3248	−23.5426
	0.06	0	−0.2240	−0.3392	−23.50
	0.08	0	−0.06685	−0.6635	−23.35
	0.10	0	−0.1333	−0.1995	−23.76
	0.11	0	0	−0.1587	−23.96
Chaotic	0.02	0.0234	0	−1.8070	−22.24
	0.14	0.08804	0	−0.2996	−23.93
	0.16	0.1536	0	−0.3062	−24.01
	0.20	0.2862	0	−0.1277	−24.36
	0.24	0.3941	0	−0.04684	−24.59
	0.26	0.4503	0	−0.03652	−24.68
Hyperchaotic	0.30	0.5050	0.05529	0	−24.86
	3	4.0530	0.09629	0	−31.15
	5	4.220	0.02539	0	−33.25
	6	4.201	0.03063	0	−34.23
	7	2.2570	0.0273	−0.1961	−33.09
	10	3.50	0.01774	−0.04853	−37.47

3.4. Varying the parameter p

Here, we fix the values the system parameters (a, b, c) as $(a, b, p) = (24, 18, 2)$ and vary the parameter p in the interval $[10, 20]$. Figure 8 shows the Lyapunov exponents spectrum and the bifurcation diagram of the 4-D system (1) when the parameter p varies in $[10, 20]$ and $(a, b, p) = (24, 18, 2)$.

It can be seen from the Figure 8 that the 4-D system (1) exhibits only hyperchaotic behavior when $p \in [10, 20]$, where $l_1 > 0$, $l_2 > 0$, $l_3 = 0$ and $l_4 < 0$.

Behaviors and Lyapunov exponents of the new 4-D system (1) for different values of parameter p are summarized in Table 4.

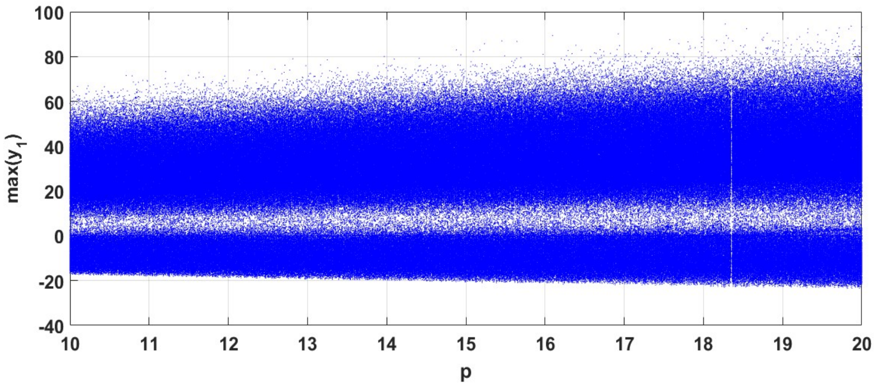

(a)

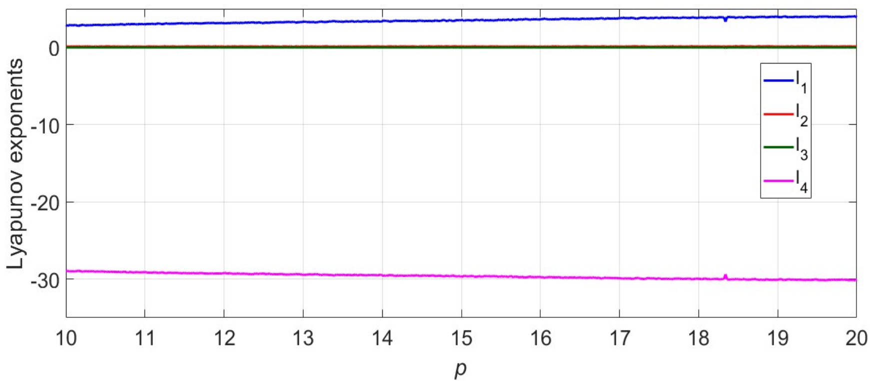

(b)

Figure 8: (a) Bifurcation diagram and (b) LE spectrum of the 4-D two-scroll dynamics (1) for $p \in [10, 20]$ and $(a, b, c) = (24, 18, 2)$

Table 4: Summary Table for the dynamic analysis of the 4-D system (1) for different values of the parameter c and $(a, b, c) = (24, 18, 2)$

Dynamics	Parameter p	LEs			
		l_1	l_2	l_3	l_4
Hyperchaotic	10	2.8980	0.09861	0	−29.00
	12	3.1070	0.08076	0	−29.19
	15	3.5590	0.1435	0	−29.71
	16	3.6630	0.1113	0	−29.78
	17	3.80	0.09241	0	−29.90
	18	3.8190	0.1323	0	−29.96
	20	3.9120	0.1069	0	−30.02

4. Multistability in the new 4-D hyperchaotic two-scroll system

A key feature of integer-order hyperchaotic systems is their ability to show multistability, meaning they can have several hyperchaotic attractors at the same time for the same parameter values. This is important for both understanding and applying hyperchaotic systems. Having multiple attractors helps reveal the system's complex behavior and makes it possible to design systems with different dynamic properties. To study the coexistence of these attractors and other system features, it's helpful to slightly change the initial conditions while keeping the system parameters fixed.

Let Y_1 and Y_2 be two different initial conditions for the new 4-D system (1), where:

$$Y_1 = (0.5, 0.5, 0.5, 0.3) \ \ \text{(blue color)}, \tag{12}$$

$$Y_2 = (-0.5, -0.3, -0.5, 1) \ \ \text{(red color)}. \tag{13}$$

We fix the values of system parameters as

$$a = 24, \ b = 18, \ c = 2, \ p = 14 \tag{14}$$

Figure 9 demonstrates the coexistence of two hyperchaotic attractors corresponding to the initial states Y_1 (blue color) and Y_2 (red color), showcasing multistability for the 4-D hyperchaotic two-scroll system (1).

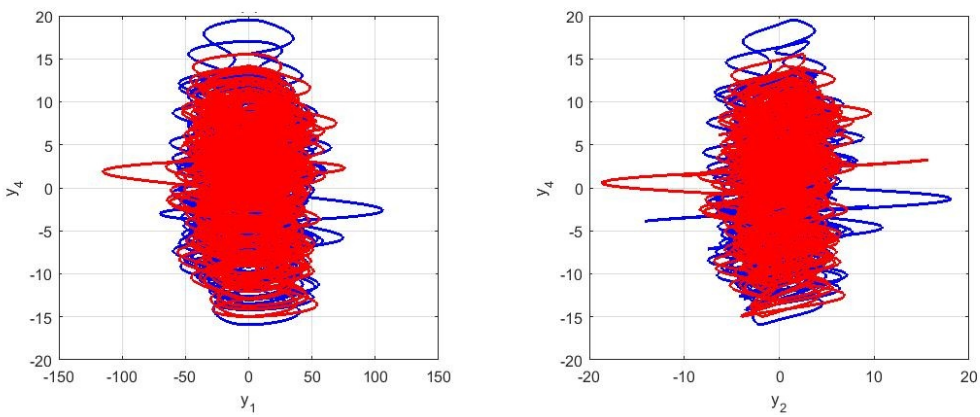

(a) (y_1, y_4) plane (b) (y_2, y_4) plane

Figure 9: Coexistence of two hyperchaotic attractors of the 4-D hyperchaotic two-scroll system (1) with different initial values where $a = 24, b = 18, c = 2, p = 14$: The initial states are chosen as $Y_1 = (0.5, 0.5, 0.5, 0.3)$ (blue orbit) and $Y_2 = (-0.5, -0.3, -0.5, 1)$ (red orbit)

5. Offset boosting control of the new hyperchaotic two-scroll system

Offset boosting control enables flexible adjustment of a system's amplitude by adding a control parameter to one of its state variables. This method does not change the system's qualitative behavior; instead, it shifts the attractor's position either positively or negatively, depending on the value of the control parameter.

The state variable y_4 appears only once in the 4-D hyperchaotic two-scroll system (1), and thus it can be easily controlled. We offset-boost the state variable y_4 by the transformation $y_4 \longrightarrow y_4 + k$, where k denotes the offset-boosting controller. The 4-D system (1) can be rewritten accordingly as follows:

$$\begin{cases} \dot{y}_1 = a(y_2 - y_1) - y_2^2 + p y_2 y_3 \,, \\ \dot{y}_2 = b y_1 - y_1 y_3 + (y_4 + k), \\ \dot{y}_3 = y_1 y_2 - c y_3 \,, \\ \dot{y}_4 = -y_1 \,. \end{cases} \tag{15}$$

When we take the parameter values as $(a, b, c, p) = (24, 18, 2, 14)$ and initial state as $y_0 = (0.5, 0.3, 0.5, 0.3)$, the offset boosted hyperchaotic attractors can be obtained for the 4-D system (15).

The 2D projection of the attractor onto (y_1, y_4) plane is shown in Figure 10b and the corresponding time-sequence diagram for the signal y_4 is given in Figure 10a.

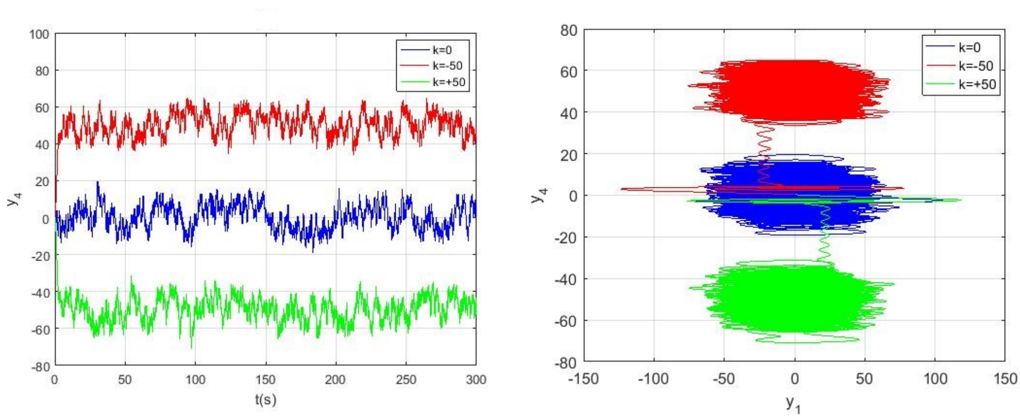

(a) (b)

Figure 10: (a) Offset chaotic signal y_4 plot and (b) Offset-boosting control of the 4-D hyperchaotic two-scroll system (15) shown in (y_1, y_4) plane with different values of parameter k, $k = -50$ (red), $k = 0$ (blue), $k = 50$ (green) in (y_1, y_4)-plane

It can be observed that a bipolar signal is obtained for $k = 0$ (blue), a unipolar signal for $k = -50$ (red), and a unipolar signal for $k = 50$ (green). Therefore, we can transform the chaotic signal y_4 from bipolarity to unipolarity when varying the control parameter k.

6. Circuit simulation of the new 4-D hyperchaotic two-scroll system

In this section, the new 4-D hyperchaotic two-scroll system (1) is realized by the NI Multisim 14.2 platform. The electronic circuit design of the 4D hyperchaotic two-scroll system (1) is shown in Figure 11 in which TLO84ACD is selected as OPAMP and the multipliers are of type AD633.

Using Kirchhoff's electrical circuit laws, we derive the circuit model for the 4D hyperchaotic two-scroll system (1) as follows:

$$\begin{cases} \dot{y}_1 = \dfrac{1}{R_1C_1}y_2 - \dfrac{1}{R_2C_1}y_1 - \dfrac{1}{R_3C_1}y_2^2 + \dfrac{1}{10R_4C_1}y_2y_3\,, \\ \dot{y}_2 = \dfrac{1}{R_5C_2}y_1 - \dfrac{1}{10R_6C_2}y_1y_3 + \dfrac{1}{R_7C_2}y_4\,, \\ \dot{y}_3 = -\dfrac{1}{R_8C_3}y_3 + \dfrac{1}{10R_9C_3}y_1y_2\,, \\ \dot{y}_4 = -\dfrac{1}{R_9C_4}y_1\,. \end{cases} \tag{16}$$

Here y_1, y_2, y_3, y_4 are the voltages across the capacitors, C_1, C_2, C_3, C_4, respectively. The values of components in the circuit are selected as follows:

$$C_1 = C_2 = C_3 = C_4 = 1 \text{ nF}, \quad R_1 = R_2 = 4.166 \text{ k}\Omega, \quad R_4 = 0.7142 \text{ k}\Omega, \tag{17}$$

$$R_3 = R_6 = R_9 = 10 \text{ k}\Omega, \quad R_5 = 5.555 \text{ k}\Omega, \quad R_7 = R_{10} = 100 \text{ k}\Omega, \tag{18}$$

$$R_8 = 50 \text{ k}\Omega, \quad R_{11} = R_{12} = R_{13} = R_{14} = R_{15} = R_{16} = 100 \text{ k}\Omega. \tag{19}$$

Multisim outputs of the 4-D hyperchaotic circuit (16) via oscilloscope XSC1 and Tektronix oscilloscope are plotted in Figures 12 to 15.

7. Complete synchronization of the new hyperchaotic two-scroll systems

This section presents a control application of the new 4-D hyperchaotic two-scroll system (1), *viz.* complete synchronization of a pair of new hyperchaotic two-scroll systems taken as the *transmitter* and *receiver* systems by means of employing the integral sliding mode control (ISMC) technique, which is a famous technique in the control literature and it has several engineering applications [35].

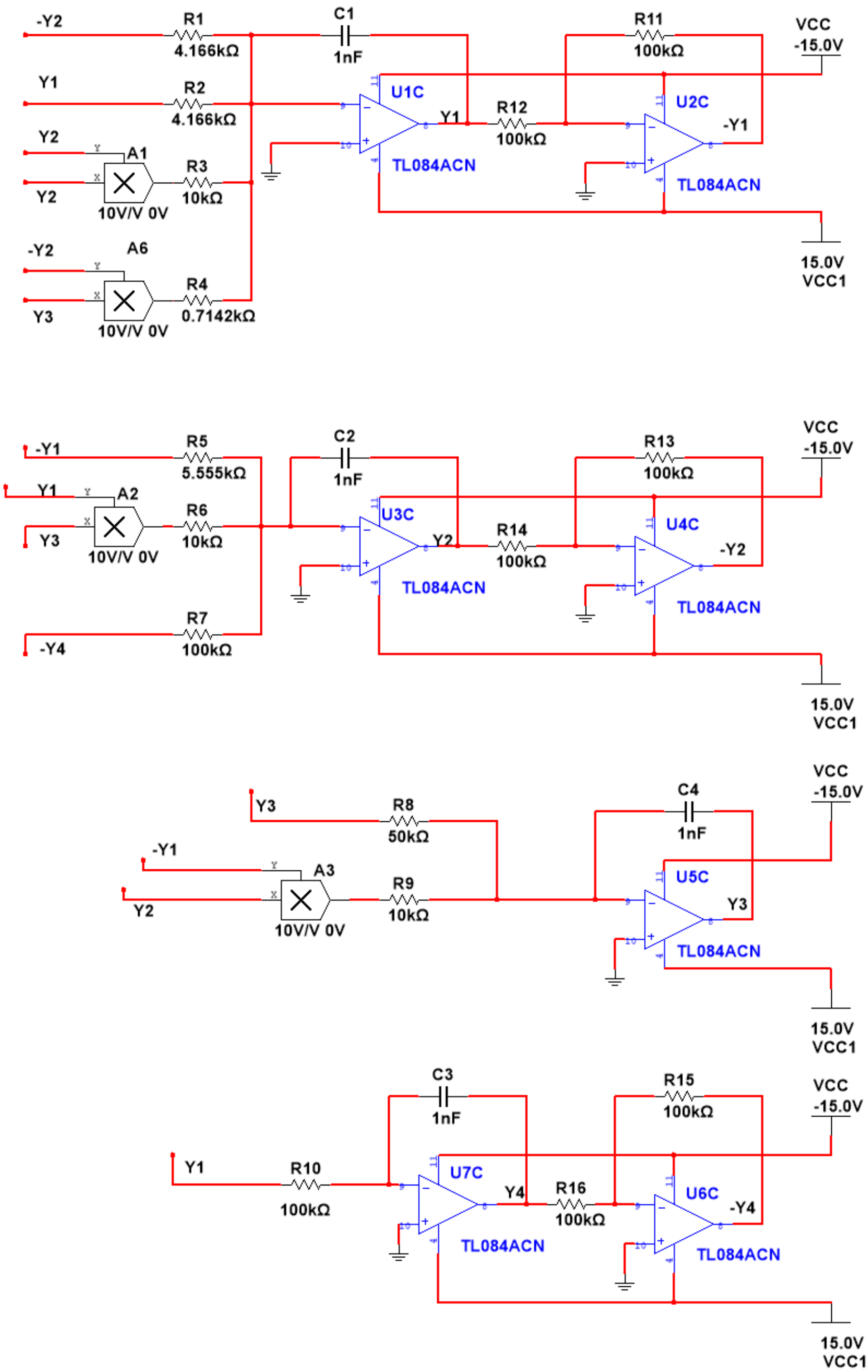

Figure 11: Circuit design of the new 4-D hyperchaotic two-scroll system (16)

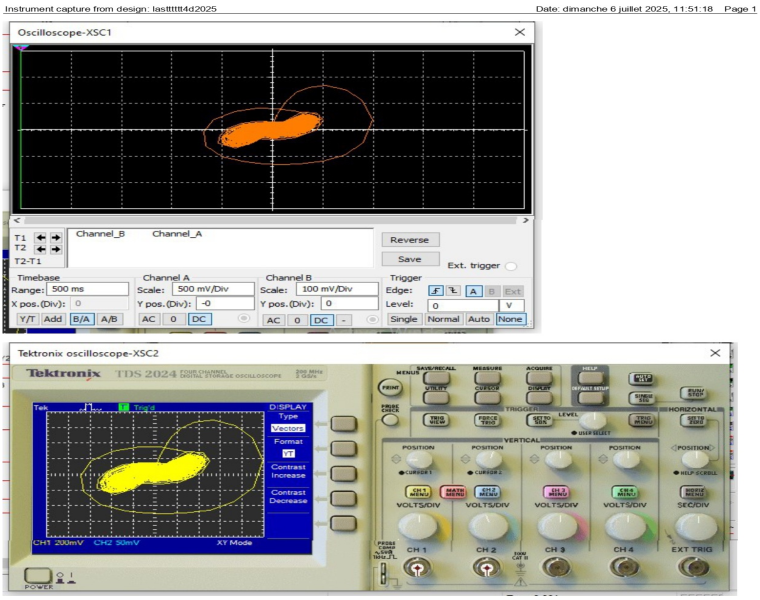

Figure 12: (y_1, y_2) plot of the new hyperchaotic system (16) via oscilloscope XSC1 and Tektronix oscilloscope

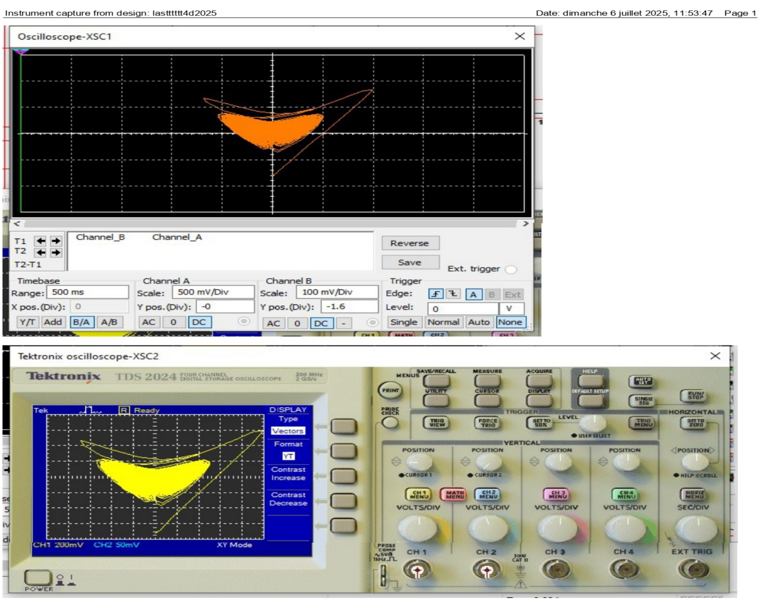

Figure 13: (y_1, y_3) plot of the new hyperchaotic system (16) via oscilloscope XSC1 and Tektronix oscilloscope

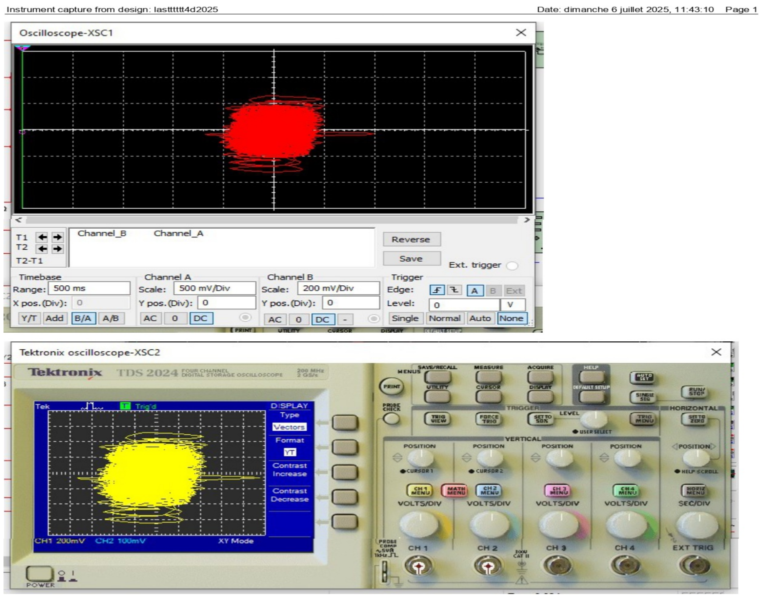

Figure 14: (y_1, y_4) plot of the new hyperchaotic system (16) via oscilloscope XSC1 and Tektronix oscilloscope

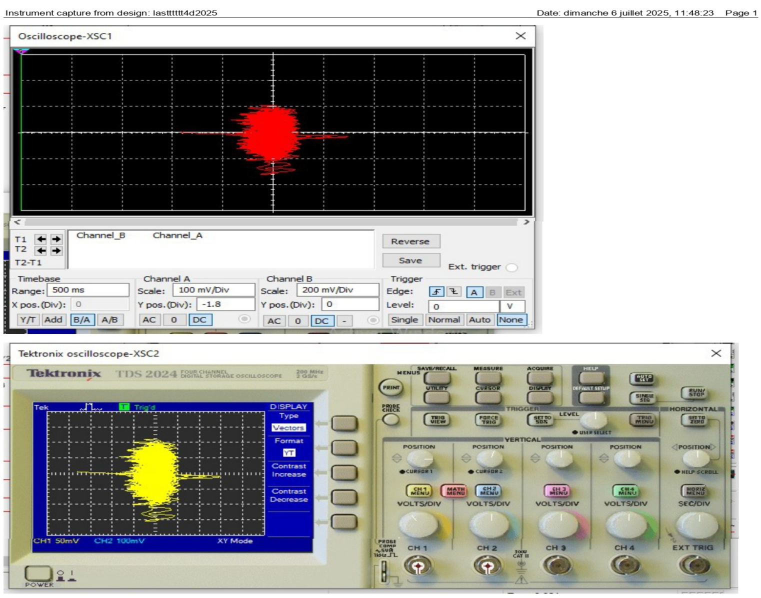

Figure 15: (y_3, y_4) plot of the new hyperchaotic system (16) via oscilloscope XSC1 and Tektronix oscilloscope

As the transmitter system, we consider the new 4-D hyperchaotic two-scroll dynamics

$$\begin{cases} \dot{z}_1 = a(z_2 - z_1) - z_2^2 + pz_2z_3 \,, \\ \dot{z}_2 = bz_1 - z_1z_3 + z_4 \,, \\ \dot{z}_3 = z_1z_2 - cz_3 \,, \\ \dot{z}_4 = -z_1 \,. \end{cases} \tag{20}$$

We denote the state of the transmitter system (20) as $Z = (z_1, z_2, z_3, z_4)$.

As the receiver system, we consider the new 4-D hyperchaotic two-scroll dynamics

$$\begin{cases} \dot{w}_1 = a(w_2 - w_1) - w_2^2 + pw_2w_3 + u_1 \,, \\ \dot{w}_2 = bw_1 - w_1w_3 + w_4 + u_2 \,, \\ \dot{w}_3 = w_1w_2 - cw_3 + u_3 \,, \\ \dot{w}_4 = -w_1 + u_4 \,. \end{cases} \tag{21}$$

We denote the state of the receiver system (21) as $W = (w_1, w_2, w_3, w_4)$.

We note that $u = (u_1, u_2, u_3, u_4)$ is the integral sliding mode controller (ISMC) which will be carefully designed so as to achieve complete synchronization between the hyperchaotic two-scroll systems (20) and (21).

We can define the complete synchronization error as follows:

$$\begin{cases} \epsilon_1 = w_1 - z_1 \,, \\ \epsilon_2 = w_2 - z_2 \,, \\ \epsilon_3 = w_3 - z_3 \,, \\ \epsilon_4 = w_4 - z_4 \,. \end{cases} \tag{22}$$

We obtain the dynamics of the synchronization error as follows:

$$\begin{cases} \dot{\epsilon}_1 = a(\epsilon_2 - \epsilon_1) - w_2^2 + z_2^2 + p(w_2w_3 - z_2z_3) + u_1 \,, \\ \dot{\epsilon}_2 = b\epsilon_1 + \epsilon_4 - w_1w_3 + z_1z_3 + u_2 \,, \\ \dot{\epsilon}_3 = -c\epsilon_3 + w_1w_2 - z_1z_2 + u_3 \,, \\ \dot{\epsilon}_4 = -\epsilon_1 + u_4 \,. \end{cases} \tag{23}$$

In the IMSC design [35], an integral sliding surfrance is assigned with each synchronization error variable ϵ_i, $(i = 1, 2, 3, 4)$ as follows:

$$\begin{cases} s_1 = \epsilon_1 + \gamma_1 \int\limits_0^t \epsilon_1(\tau)\mathrm{d}\tau, \\ s_2 = \epsilon_2 + \gamma_2 \int\limits_0^t \epsilon_2(\tau)\mathrm{d}\tau, \\ s_3 = \epsilon_3 + \gamma_3 \int\limits_0^t \epsilon_3(\tau)\mathrm{d}\tau, \\ s_4 = \epsilon_4 + \gamma_4 \int\limits_0^t \epsilon_4(\tau)\mathrm{d}\tau. \end{cases} \tag{24}$$

A simple calculation results in the following dynamics:

$$\begin{cases} \dot{s}_1 = \dot{\epsilon}_1 + \gamma_1\epsilon_1 , \\ \dot{s}_2 = \dot{\epsilon}_2 + \gamma_2\epsilon_2 , \\ \dot{s}_3 = \dot{\epsilon}_3 + \gamma_3\epsilon_3 , \\ \dot{s}_4 = \dot{\epsilon}_4 + \gamma_4\epsilon_4 . \end{cases} \tag{25}$$

We consider the integral sliding mode controls defined as follows:

$$\begin{cases} u_1 = -a(\epsilon_2 - \epsilon_1) + w_2^2 - z_2^2 - p(w_2w_3 - z_2z_3), \\ \qquad - \gamma_1\epsilon_1 - \beta_1 \operatorname{sgn}(s_1) - K_1s_1 , \\ u_2 = -b\epsilon_1 - \epsilon_4 + w_1w_3 - z1z_3 - \gamma_2\epsilon_2 - \beta_2 \operatorname{sgn}(s_2) - K_2s_2 , \\ u_3 = c\epsilon_3 - w_1w_2 + z_1z_2 - \gamma_3\epsilon_3 - \beta_3 \operatorname{sgn}(s_3) - K_3s_3 , \\ u_4 = \epsilon_1 - \gamma_4\epsilon_4 - \beta_4 \operatorname{sgn}(s_4) - K_4s_4 . \end{cases} \tag{26}$$

In Eq. (26), β_i, γ_i, K_i, $(i = 1, 2, 3, 4)$ are chosen to be positive constants. From (23) and (26), we obtain the closed-loop error dynamics as follows:

$$\begin{cases} \dot{\epsilon}_1 = -\gamma_1\epsilon_1 - \beta_1 \operatorname{sgn}(s_1) - K_1s_1 , \\ \dot{\epsilon}_2 = -\gamma_2\epsilon_2 - \beta_2 \operatorname{sgn}(s_2) - K_2s_2 , \\ \dot{\epsilon}_3 = -\gamma_3\epsilon_3 - \beta_3 \operatorname{sgn}(s_3) - K_3s_3 , \\ \dot{\epsilon}_4 = -\gamma_4\epsilon_4 - \beta_4 \operatorname{sgn}(s_4) - K_4s_4 . \end{cases} \tag{27}$$

The main control result for the synchronization of master-slave hyperchaotic systems (20) and (21) using the integral sliding mode control (ISMC) can be stated as follows.

Theorem 1. *The integral sliding mode control (ISMC) law stated in the equation (26) achieves complete global hyperchaos synchronization between the transmitter two-scroll system (20) and the receiver two-scroll system (21) for all values of the initial states* $Y(0), W(0) \in \mathbf{R}^4$, *where* β_i, γ_i, K_i, $(i = 1, 2, 3, 4)$ *are chosen as positive constants.*

Proof. We use Lyapunov stability theory to prove this result.

We take the Lyapunov function defined by

$$V(s_1, s_2, s_3, s_4) = \frac{1}{2}\left(s_1^2 + s_2^2 + s_3^2 + s_4^2\right). \tag{28}$$

It is easy to see that V is a quadratic and strictly positive definite function on $\mathbf{R}^4$.

A direct calculation shows that

$$\dot{V} = \sum_{i=1}^{4} s_i \left(-\beta_i \text{sgn}(s_i) - K_i s_i\right). \tag{29}$$

Simplifying the equation (29), we get

$$\dot{V} = -\sum_{i=1}^{4} \left(\beta_i |s_i| + K_i s_i^2\right). \tag{30}$$

Since β_i and K_i are positive constants for $i = 1, 2, 3, 4$, we deduce from the equation (30) that $\dot{V}$ is a strictly negative definite function defined on $\mathbf{R}^4$.

Using Lyapunov stability theory, we deduce that $s_i(t) \to 0$ as $t \to \infty$ for $i = 1, 2, 3, 4$.

Hence, it follows that $\epsilon_i(t) \to 0$ as $t \to \infty$ for $i = 1, 2, 3, 4$.

This completes the proof.

For numerical simulations in MATLAB, we take the parameter values as in the hyperchaotic case, *viz.*

$$a = 24, \quad b = 18, \quad c = 2, \quad p = 14. \tag{31}$$

We take the values of ISMC parameters as follows:

$$\beta_1 = 0.5, \quad \beta_2 = 0.5, \quad \beta_3 = 0.5, \quad \beta_4 = 0.5, \quad \gamma_1 = 6, \quad \gamma_2 = 6, \tag{32}$$

$$\gamma_3 = 6, \quad \gamma_4 = 6, \quad K_1 = 12, \quad K_2 = 12, \quad K_3 = 12, \; K_4 = 12. \tag{33}$$

The initial state of the transmitter system (20) is taken as follows:

$$z_1(0) = 1.5, \quad z_2(0) = 7.6, \quad z_3(0) = 6.8, \quad z_4(0) = 2.9. \tag{34}$$

The initial state of the receiver system (21) is taken as follows:

$$w_1(0) = 5.7, \quad w_2(0) = 3.2, \quad w_3(0) = 0.4, \quad w_4(0) = 7.5. \tag{35}$$

Figure 16 depicts the time-history of the synchronization error between the transmitter two-scroll system (20) and the receiver two-scroll system (21).

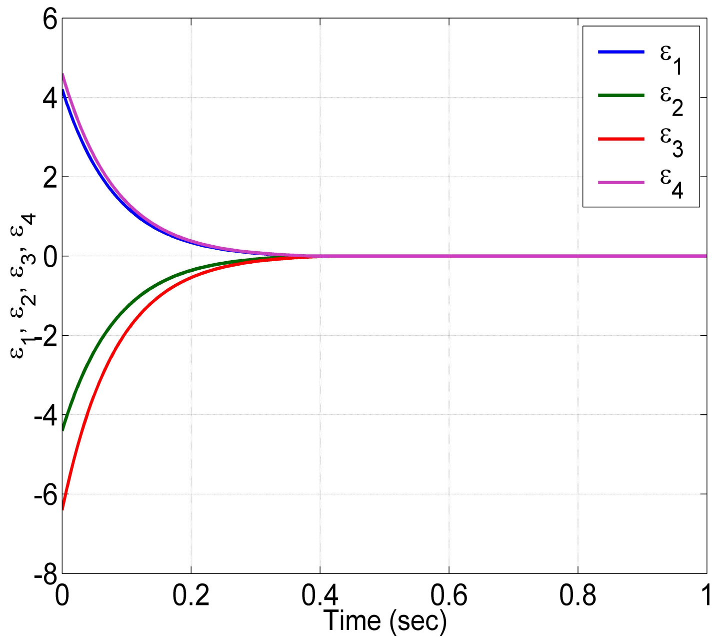

Figure 16: Time-history of the synchronization error between the transmitter two-scroll system (20) and the receiver two-scroll system (21)

8. Conclusions

The main contribution of this research work is the modelling of a new hyperchaotic two-scroll system with two unstable equilibrium points. By carrying out a rigorous dynamic analysis, we detailed the qualitative properties of the new hyperchaotic system such as the equilibrium points of the system, phase portraits, Lyapunov exponents, Lyapunov dimension, etc. We performed a detailed bifurcation analysis for the proposed hyperchaotic two-scroll system by varying the system parameters. Multistability property of the new hyperchaotic two-scroll system was also illustrated by showing the coexistence of hyperchaotic attractors for the proposed hyperchaotic two-scroll system for the same set of parameter values but different initial conditions. For engineering applications, we exhibited an electronic circuit simulation of the proposed hyperchaotic two-scroll system using MultiSim 14.0. Finally, as a control application, we derived new results for the complete synchronization for a pair of new hyperchaotic two-scroll systems taken as the master and slave systems. We applied integral sliding mode control (ISMC) and Lyapunov stability theory for the derivation of the synchronizing control law for the complete synchronization design for a pair of new hyperchaotic two-scroll systems. We used MATLAB to illustrate all the main results of this work.

References

[1] S. Vaidyanathan and A.T. Azar: *Backstepping Control of Nonlinear Dynamical Systems,* Academic Press, New York, 2020.

[2] Q. Wan, C. Chen, T. Liu, H. Rao and J. Dong: High-dimensional memristor-coupled multiple neural networks with spatial multi-structure attractors and application in image encryption. *Chaos, Solitons & Fractals,* **199**(1), (2025). DOI: 10.1016/j.chaos.2025.116716

[3] F. Meng, G. Wu and J. Zang: A novel color image encryption algorithm based on fractional-order conservative memristive hyperchaotic system and extended zig-zag transform. *Journal of King Saud University – Computer and Information Sciences,* **37**(6), (2025). DOI: 10.1007/s44443-025-00163-7

[4] E.A. Umoh and O.J. Tola: Robust global synchronization of a hyperchaotic system with wide parameter space via integral sliding mode control technique. *International Journal of Robotics and Control Systems,* **1**(4), (2011), 453–462. DOI: 10.31763/ijrcs.v1i4.485

[5] C. Medina Galindo Ana, C.A. Liliana, G.R.M. Lopez and C.H. Cesar: Flocking behavior of boids driven by hyperchaotic MACM system. *Chaos Theory and Applications,* **6**(2), (2024), 152–158. DOI: 10.51537/chaos.1376145

[6] Y. Shen, Z. Chen, Y. LI and W. LI: Coexisting attractors, amplitude control, circuit implementation of grid-scroll memristive hyperchaotic oscillator and its application in underwater signal detection. *Mechanical Systems and Signal Processing,* **25**, (2025). DOI: 10.1016/j.ymssp.2025.112525

[7] Y. Yang, L. Huang, X. Yu, N.V. Kuznetsov and Q. Lai: Generating multi-wing hidden hyperchaotic attractors with a single stable equilibrium. *IEEE Transactions on Circuits and Systems II: Express Briefs,* **71**(4), (2025), 2374–2378. DOI: 10.1109/TCSII.2023.3335096

[8] S. Rajendran and P. Kaliyaperumal: Prescribed-time synchronization of hyperchaotic fuzzy stochastic PMSM model with an application to secure communications. *Applied Mathematics and Computation,* **493**, (2025). DOI: 10.1016/j.amc.2024.129257

[9] Y. Ai, Z. Feng and H. Wang: Fixed-time adaptive fuzzy anti-synchronization control of hyperchaotic Rössler system based on backstepping method. *International Journal of Fuzzy Systems,* **25**(6), (2023), 2501–2513. DOI: 10.1007/s40815-023-01536-8

[10] M.D. Johansyah, S.M. Hamidzadeh, K. Benkouider, S. Vaidyanathan, A. Sambas, M.A. Mohamed and A.A. Aziz: A novel hyperchaotic financial system with sinusoidal hyperbolic nonlinearity: From theoretical analysis to adaptive neural fuzzy controller method. *Chaos Theory and Applications,* **6**(1), (2024), 26–40. DOI: 10.51537/chaos.1336838

[11] M. Haris, M. Shafiq, I. Ahmad, Z. Ali, G. Manickam and A. Ghaffar: A time-efficient nonlinear control method for the hyperchaotic finance system synchronization. *Indonesian Journal of Electrical Engineering and Computer Science,* **35**(2), (2024), 834–843. DOI: 10.11591/ijeecs.v35.i2.pp834-843

[12] H.A. Abdulkadhim and J.N. Shehab: Audio steganography based on least significant bits algorithm with 4D grid multi-wing hyper-chaotic system. *International Journal of Electrical and Computer Engineering,* **12**(1), (2022), 320–330. DOI: 10.11591/ijece.v12i1.pp320-330

[13] M. Tian, Y. Cui, Z. Liu and H. Chen: Optical audio cryptosystem using hyperchaotic implementation in Gyrator domain. *Physics Open,* **23**, (2025). DOI: 10.1016/j.physo.2025.100264

[14] Y. Lalili, T. Bouden, M. Grimes, M.E. Yalcin, L. Abderraza and E. Elbasi: FPGA realization of a controllable 4-D hyperchaotic system for quantum-inspired medical image encryption. *Physica Scripta,* **100**, (2025). DOI: 10.1088/1402-4896/adea21

[15] X. Qin and Y. Zhang: Image encryption algorithm based on COA and hyperchaotic Lorenz system. *Nonlinear Dynamics,* **112** (2024), 10611–10632. DOI: 10.1007/s11071-024-09632-6

[16] F. Zhang, S. Chen, X. Chen, F. Xu and M. Xiao: Qualitative behaviors and control of a new four-dimensional Lorenz system. *Journal of Applied Analysis and Computation,* **15**(5), (2025), 3025–3044. DOI: 10.11948/20240462

[17] S. Vaidyanathan, I.M. Moroz, A. Sambas, M.A. Mohamed, M. Mamat and M.Z. Ahmad: A new multistable 4-D hyperchaotic four-scroll system, its dynamic analysis and circuit design. *Engineering Letters,* **29**(4), (2021), 1311–1318.

[18] K.S. Ojo, A.B. Adeloye and A.O. Busari: Switching tracking control and synchronization of four-scroll hyperchaotic systems. *Journal of Applied Nonlinear Dynamics,* **7**(4), (2018), 329–335. DOI: 10.5890/JAND.2018.12.001

[19] T. Zhao, Y. Wei, X. Wang, X. Sun and B. Du: A novel conservative grid multi-scroll hyperchaotic system with two-parameter regulation. *European Physical Journal Plus,* **140**(6), (2025). DOI: 10.1140/epjp/s13360-025-06487-7

[20] Y. Li and M. Li: Analysis and implementation of a novel parametrically controllable spherical multi-scroll memristive conservative hyperchaotic system. *Integration,* **103**, (2025). DOI: 10.1016/j.vlsi.2025.102409

[21] L.J. Sagban and A.A. Shukur: Dynamics and adaptive control of a novel 5D hyperchaotic system: Either hidden attractor or self-excited with unusual nature of unstable equilibria. *Malaysian Journal of Mathematical Sciences,* **18**(3), (2024), 675–696. DOI: 10.47836/mjms.18.3.14

[22] V.-T. Pham, S. Vaidyanathan, C. Volos and T. Kapitaniak: *Nonlinear Dynamical Systems with Self-Excited and Hidden Attractors,* Springer, Berlin, Germany, 2018.

[23] A. Gokyildirim, U.E. Kocamaz and H. Calgan: A novel five-term 3D chaotic system with two squared nonlinearities and its secure communication application for biomedical data. *Biomedical Signal Processing and Control,* **112**, (2026). DOI: 10.1016/j.bspc.2025.108494

[24] S. Hu and L. Zhou: Stochastic Hopf bifurcation and random chaos of a multi-stable rotational energy harvesting system. *Chaos, Solitons and Fractals,* **199**, (2025). DOI: 10.1016/j.chaos.2025.116850

[25] N. Wang, Y. Lv, H. Bao, S. Zhao and Q. Xu: Fractal-induced multistability in Chua's circuit. *Chaos, Solitons and Fractals,* **200**, (2025). DOI: 10.1016/j.chaos.2025.116939

[26] Z. Yang, B. Zhou, D. Li, X. Li and W. Zhang: Global dynamics and multistability in a class of piecewise asymmetric oscillators. *Journal of Computational and Nonlinear Dynamics,* **20**(10), (2025). DOI: 10.1115/1.4068977

[27] Y. Zhou, R. Li and Z. Cui: Dynamics, circuit simulation and fixed-time projection synchronization in a memristor-based hyperchaotic system. *Symmetry,* **17**(5), (2025). DOI: 10.3390/sym17050685

[28] K. Zourmba, B. Fu and K. Sun: Dynamics and circuit implementation of a novel coupled discrete memristive system. *Integration*, **105**, (2025). DOI: 10.1016/j.vlsi.2025.102504

[29] S. Vaidyanathan and A.T. Azar: Dynamic analysis, adaptive feedback control and synchronization of an eight-term 3-D novel chaotic system with three quadratic nonlinearities. *Studies in Intelligence,* **337**, (2016), 155–178. DOI: 10.1007/978-3-319-30340-6_7

[30] A. Ouannas, A.T. Azar and S. Vaidyanathan: A robust method for new fractional hybrid chaos synchronization. *Mathematical Methods in the Applied Sciences,* **40**(5), (2017), 1804–1812. DOI: 10.1002/mma.4099

[31] X. An, Z. Li, L. Jiang, L. Xiong and J. Zhang: Synchronization and energy control for a class of electro-mechanical system coupled with piezoelectric neural circuit. *Applied Mathematical Modelling,* **147**, (2025). DOI: 10.1016/j.apm.2025.116203

[32] X. Wu and S. Yan: Adaptive sliding mode synchronization of a controllable grid-multi-wing chaotic system with parameter identification. *Applied Mathematical Modelling,* **150**, (2026). DOI: 10.1016/j.apm.2025.116351

[33] M. Hui and J. Yan: Integral sliding mode exponential synchronization of inertial memristive neural networks with time varying delays. *Neural Processing Letters,* **55**(3), (2023), 2725–2742. DOI: 10.1007/s11063-022-10981-9

[34] S. Vaidyanathan, I.M. Moroz and A. Sambas: A new two-scroll 4-D hyperchaotic system with a unique saddle point equilibrium, its bifurcation analysis, circuit design and a control application to complete synchronization. *Archives of Control Sciences,* **33**(2), (2023), 277–298. DOI: 10.24425/acs.2023.146276

[35] S. Vaidyanathan and C.H. Lien: *Applications of Sliding Mode Control in Science and engineering.* Springer, Berlin, Germany, 2017.